$F_2H)_4$. According to the NMR data, all of the PF_2H was consumed, which is reasonable considering that side reactions involving PF_2H are seen at −80 °C. $Ni(PF_2H)_4$ can be isolated from the various byproducts by vacuum manipulation if desired. In our hands, the bis(allyl)nickel route to $Ni(PF_2H)_4$ is superior to the metal atom reactor route described earlier.

Synthesis of $Fe(PF_3)_5$

A 2-mmol sample of $Fe(C_5H_7)_2$ was placed in the reaction tube and dissolved in about 25 mL of hexane. The reaction tube consisted of a 100-mL heavy-walled Pyrex tube fitted with a stainless steel cap and valve (Fischer & Porter Co.). The solution was degassed and frozen at −196 °C under vacuum. Approximately 20 mmol of PF_3 was then condensed into the tube. This would generate a pressure of approximately 5 atm in 100 mL at room temperature. After the tube was removed from the liquid-nitrogen bath, it was placed in a wire mesh pouch and placed behind a safety shield. The mixture was then heated to approximately 60 °C and stirred for 1 day. The reaction mixture was sampled, and $Fe(PF_3)_5$ was identified as the only observable product by ^{31}P NMR.[17]

Acknowledgment. Support of this work by the National Science Foundation through Grant Nos. CHE 7920313 and CHE 8120683 and by the donors of the Petroleum Research Fund, administered by the American Chemical Society, is gratefully acknowledged.

Registry No. $Ni(PF_3)_4$, 13859-65-9; $Fe(PF_3)_5$, 13815-34-4; $Ni(PF_2H)_4$, 69814-91-1; $Ni(PCl_3)_4$, 36421-86-0; $Ni(PF_2N(CH_3)_2)_4$, 15053-92-6; $Ni(PF_2Cl)_4$, 15024-22-3; NiB_2 (B = allyl), 12077-85-9; bis(pentadienyl)iron, 74910-62-6.

(17) Kruck, Th.; Prasch, A. *Z. Anorg. Allg. Chem.* **1968**, *356*, 128.

Department of Chemistry
University of Utah
Salt Lake City, Utah 84112

Sarah J. Severson
Teddy H. Cymbaluk
Richard D. Ernst
John M. Higashi
Robert W. Parry*

Received September 9, 1983

Articles

Contribution from the Department of Chemistry,
Texas A&M University, College Station, Texas 77843

Silver Clusters in Zeolites: Fenske–Hall Self-Consistent Field Molecular Orbital Calculations

ROBERT A. SCHOONHEYDT,*[1] MICHAEL B. HALL, and JACK H. LUNSFORD

Received March 25, 1983

The Fenske–Hall SCF–MO calculation was applied to Ag, Ag_2, and Ag_3 and the same clusters in a zeolitic environment. The spectroscopic properties of the naked clusters were calculated by using variable 5s and 5p exponents in the Slater-type 5s and 5p orbitals. For the calculation of the spectra of these clusters in the zeolites it is necessary to use Ag^+ functions. It is shown that the 5s–5p transition of Ag^0 in site I of zeolites X and Y occurs at almost the same position as in the gas phase. The yellow color of fully Ag-exchanged zeolites X and Y is due to a charge-transfer transition from Ag^0 on sites I′ to Ag^+ on site I. The calculations do not allow one to distinguish between dinuclear and trinuclear clusters. The most probable charge on the clusters is 1+. The yellow color of zeolite A is due to a charge transfer from the central Ag to the external Ag in the cluster Ag^+–Ag^0–Ag^+.

Introduction

Ag^+-exchanged zeolites form Ag clusters upon dehydration (zeolite A) or upon dehydration and oxidation (faujasite-type zeolites). Three types of clusters have been proposed on the basis of X-ray diffraction data.[2-4] In zeolite A Ag atoms form a linear cluster with a nuclearity of 3 inside the cubooctahedron.[3] The two external Ag atoms are coordinated to the three O_3 oxygens of the hexagonal ring with an interatomic distance of 0.223 nm. The central Ag occupies a site opposite the four-membered framework ring at a distance of 0.270 nm. The Ag–Ag distance is 0.285–0.300 nm, to be compared to the 0.289 nm in Ag metal.[5] Because of these interatomic distances the cluster is formally written as Ag^+–Ag^0–Ag^+. A maximum number of four Ag_3^{2+} clusters can be accommodated in one cubooctahedron, giving a cluster ($Ag_4^0Ag_8^{8+}$) very similar to the (Ag_6^0)(Ag_8^{8+}) cluster proposed by Seff.[2] In faujasite-type zeolites simultaneous occpancy of sites I and I′[6] by Ag was detected by X-ray diffraction.[4] The Ag–Ag distance is then 0.312 nm. Thus, cluster formation may be proposed. The charge of these clusters and their nuclearity are, however, ill-defined.[4] For Y-type zeolite, the excess occupancy of sites I and I′ can, in principle, be explained by dinuclear clusters. In X-type zeolites, trinuclear clusters must be assumed.[4]

The formation of these clusters is accompanied by a yellow coloration of the zeolites, and for interacting clusters in zeolite A, a brick red color is developed. These colors are due to visible absorption band at 25 000 cm^{-1} (3.10 eV) (yellow faujasite-type zeolites), at 23 000 cm^{-1} (2.85 eV) (yellow zeolite A) and at 20 000 cm^{-1} (2.48 eV) (brick red zeolite A).[3,7] For the faujasite-type zeolites bands at 30 100 ± 600 cm^{-1} (3.73 eV) and at 29 400 cm^{-1} (3.65 eV) of 27 800 cm^{-1} (3.45 eV)

(1) Present address: Centrum voor Oppervlaktescheikunde en Colloïdale Scheikunde, Katholieke Universiteit Leuven, De Croylaan 42, B-3030 Leuven (Heverlee), Belgium.
(2) Kim, Y.; Gilje, J. W.; Seff, K. *J. Am. Chem. Soc.* **1977**, *99*, 7005. Kim, Y.; Seff, K. *Ibid.* **1978**, *100*, 175.
(3) Gellens, L. R.; Mortier, W. J.; Schoonheydt, R. A.; Uytterhoeven, J. B. *J. Phys. Chem.* **1981**, *85*, 2783.
(4) Gellens, L. R.; Mortier, W. J.; Uytterhoeven, J. B. *Zeolites* **1981**, *1*, 11, 85.
(5) "Handbook of Chemistry and Physics", 52nd ed.; Chemical Rubber, Publishing Co.: Cleveland, OH, 1971; p F174.
(6) The site notation is as follows: site I = hexagonal prism; site I′ = inside the cubooctahedron on the hexagonal rings of the hexagonal prism. Ag(I) denotes Ag in the hexagonal prism or in site I; Ag(I′) denotes Ag in site I′.
(7) Gellens, L. R.; Schoonheydt, R. A. In "Metal Microstructures in Zeolites"; Jacobs, P. A., Jaeger, N. I., Jiru, P., Schulz-Ekloff, G., Eds.; Elsevier: Amsterdam, 1982; p 87.

0020-1669/83/1322-3834$01.50/0

Table I. Interatomic Distances Selected for the Calculation of Ag Clusters in Zeolites

faujasite-type zeolites		zeolite A	
bond type	bond length/nm	bond type	bond length/nm
Ag-Ag	0.312	Ag-Ag	0.289
Ag(I)-O(3)	0.257	Ag-O(3)	0.223
Ag(I')-O(3)	0.266		

are ascribed respectively to Ag^0 in the hexagonal prisms and Ag_2^+ in Y-type and in X-type zeolites.[7-9]

The interpretation of these spectral data in terms of the cluster models proposed on the basis of the X-ray diffraction data is not straightforward. With an extended Hückel calculation Gellens et al[10] showed that the interaction of Ag_3 clusters with the zeolitic framework was very weak, but they failed to explain the visible absorption bands. Ozin[11] proposed that the 25 000-cm^{-1} band of the yellow faujasite-type zeolites was due to a transition from filled molecular orbitals of 4d character to the singly occupied $3\sigma_g^+$ orbital of 5s character of the cluster Ag_3^{2+}. The bands of Ag^0 and Ag_2^+, however, are interpreted as 5s → 5p transitions.[11]

These interpretations are based on the vast literature of matrix-isolated Ag clusters, on Xα calculations of the naked clusters, and on the interpretation of the emission spectra of the zeolite-supported Ag clusters.[11-14] With this background information an attempt to relate the spectral data to the electronic properties of the proposed Ag clusters in zeolites is worthwhile, if the zeolitic environment is included in the calculations. We have done this with the Fenske–Hall self-consistent field calculational procedure.[15] This paper reports the results.

Computational Procedures

The Fenske–Hall SCF calculational procedure was applied. Computational details have been published.[15] The energy levels of the MO's constructed from the atomic valence orbitals are obtained self-consistently without the introduction of adjustable parameters. The results depend only on the choice of the atomic basis functions and the internuclear distances.

Atomic Basis Functions. Analytical wave functions for Ag ($4d^{10}5s$) and O are taken from Roetti and Clementi.[16] Atomic orbitals are derived as linear combinations of Slater-type functions by curve fitting according to the maximum overlap criterion. All the atomic orbitals are orthonormalized. The valence orbital set of Ag is taken as (4d 5s 5p). The exponents of the 5s and 5p Slater-type functions of Ag are considered as variables. They are chosen so as to fit the experimental gas-phase spectra of Ag, Ag_2, and Ag_3.[17,18] These 5s and 5p functions are then used to calculate the energy levels of Ag, Ag_2, and Ag_3 in the zeolitic matrix. Ag^+ functions are also used in the calculations.[19] In this case, the exponents of the 5s and 5p functions used to set up the 5s and 5p atomic orbitals are given the value 2.0. The physical reasoning behind the use of Ag^+ functions is that the valence orbitals of Ag in a bonding situation will be considerably contracted, resembling more those of Ag^+ than those of the naked Ag atom. This extreme situation probably does not occur in the inert-gas matrices, usually used to study small metal clusters, but is expected in the more polar zeolite environment.

Table II. Calculated Transitions of Ag_3

Ag functions		Ag^+ functions	
energies/eV	assignt	energies/eV	assignt
0.67	$1\sigma_g \rightarrow 1\sigma_u$	0.68	$1\sigma_g \rightarrow 1\sigma_u$
2.58	$1\sigma_u \rightarrow 2\sigma_g$	1.95	$1\sigma_u \rightarrow 2\sigma_g$
3.41	$1\sigma_g \rightarrow 2\sigma_u$	4.05	$1\sigma_g \rightarrow 2\sigma_u$
4.44	$1\sigma_u \rightarrow \pi_g$	4.87	$1\sigma_u \rightarrow \pi_g$
4.58	$1\sigma_g \rightarrow 1\pi_u$	5.48	$1\sigma_g \rightarrow 1\pi_u$
6.56	$1\sigma_g \rightarrow 2\pi_u$	5.84	$1\sigma_g \rightarrow 2\pi_u$

Table III. Atomic Charges on the Atoms of Ag_3

	charges	
	central Ag	external Ag
Ag functions	0.24−	0.12+
Ag^+ functions	0.08−	0.04+

Models. To simulate the zeolitic environment, Ag, Ag_2, and Ag_3 are surrounded by H_2O molecules. The number of H_2O molecules equals the number of nearest-neighboring lattice oxygens of the zeolites as determined by X-ray diffraction.[3,4] The coordinates of the Ag and O atoms are taken from the X-ray diffraction studies. As a consequence the Ag–O and Ag–Ag distances are those occurring in zeolites. They are summarized in Table I.

The following models have been considered: (i) Ag^0 in the hexagonal prisms (model 1); (ii) $Ag_2^{0,+}$ with one Ag in the hexagonal prism and one Ag on an adjacent site I′ (model 2); (iii) linear $Ag^{0,+,2+}$ with one Ag in the hexagonal prism and 2 Ag's on the adjacent sites I′ (model 3); (iv) linear $Ag_3^{0,+,2+}$ in the cubooctahedron with the external Ag atoms facing the hexagonal rings (model 4). The first three models refer to faujasite-type zeolites. The first coordination sphere is made up of six O_3 atoms of the hexagonal prisms. The central Ag, or Ag in site I, is coordinated to these six oxygens; the Ag atoms in site I′ are coordinated to three O_3 atoms. The fourth model is appropriate for zeolite A. The external Ag atoms are coordinated to three O_3 atoms of the hexagonal rings. The central Ag is coordinated only to the two external Ag atoms.

These H_2O models may seem poor models for a zeolitic environment. There are 3 reasons for this choice: (i) The cluster-framework interaction is very weak.[10] (ii) The energy levels of interest are almost purely Ag levels whatever the size and the charge of the clusters. (iii) We do not expect to obtain a unique quantitative picture of the spectral properties of Ag clusters in zeolites with this type of calculation. Rather, we want (a) to show if the models proposed in the literature on the basis of X-ray diffraction data are reasonable and (b) to give a qualitative interpretation of the spectral properties of zeolitic Ag clusters. The results show that we have succeeded in these two goals.

Results

1. Ag, Ag_2, and Ag_3. The exponents of the 5s and 5p Slater-type functions are adapted to fit the calculated transitions of Ag, Ag_2, and Ag_3 to the experimental gas-phase spectra.[17,18] In the case of Ag^0 the $^2S_{1/2} \rightarrow {}^2P_{1/2}$ transition at 3.66 eV is exactly calculated with 5s and 5p exponents of 1.522 and 1.805, respectively. But 5s exponents in the range 1.522–1.940 combined with 5p exponents in the range 1.720–1.850 give transition energies in the range 3.39–3.61 eV. In view of the approximate nature of the calculation all these exponents adequately describe the Ag spectrum.

Ag_2 is characterized by two transitions: $^1\Sigma_g^+ \rightarrow {}^1\Sigma_u^+$ at 2.85 eV and $^1\Sigma_g^+ \rightarrow {}^1\Pi_u$ at 4.41 eV.[18] A reproduction of these transition energies within 0.30 eV is possible with 5s exponents in the range 1.700–1.940 combined with 5p exponents in the range 1.720–1.830.

The experimental gas-phase spectrum of Ag_3 consists of a band at 2.59 eV and a triplet in the range 4.67–4.98 eV.[18] The former is identified as the $^2\Sigma_u^+ \rightarrow {}^2\Sigma_g^+$ transition ($1\sigma_u \rightarrow 2\sigma_g$), but the nature of the triplet is unclear at this moment.[13] Figure 1 shows the results of two of our calculations. In Figure 1A we have used Ag functions with the exponents of the 5s and

(8) Kellerman, R.; Texter, J. *J. Chem. Phys.* **1979**, *70*, 1562.
(9) Ozin, G. A.; Hughes, F. *J. Phys. Chem.* **1983**, *87*, 94.
(10) Gellens, L. R.; Mortier, W. J.; Lissillour, R.; Le Beuze, A. *J. Phys. Chem.* **1982**, *86*, 2509.
(11) Ozin, G. A.; Hughes, F.; McIntoch, D. F. In "Intrazeolitic Chemistry"; American Chemical Society: Washington, DC, 1983; ACS Symp. Ser. No. 218, p 409.
(12) For a review see: Ozin, G. A. *Symp. Faraday Soc.* **1980**, *14*, 7.
(13) Basch, H. *J. Am. Chem. Soc.* **1981**, *103*, 4657.
(14) Ozin, G. A.; Huber, H.; McIntosch, D.; Mitchell, S.; Norman, J. G., Jr.; Noodleman, L. *J. Am. Chem. Soc.* **1979**, *101*, 3504.
(15) Hall, M. B.; Fenske, R. F. *Inorg. Chem.* **1972**, *11*, 768.
(16) Roetti, C.; Clementi, E. *J. Chem. Phys.* **1974**, *60*, 3342.
(17) Brewer, L.; King, B. A.; Wang, J. L.; Meyer, B.; Moore, G. F. *J. Chem. Phys.* **1968**, *49*, 5209.
(18) Schulze, W.; Abe, H. *Symp. Faraday Soc.* **1980**, *14*, 87.
(19) Ag^+ functions were kindly supplied by Prof. M. B. Hall.

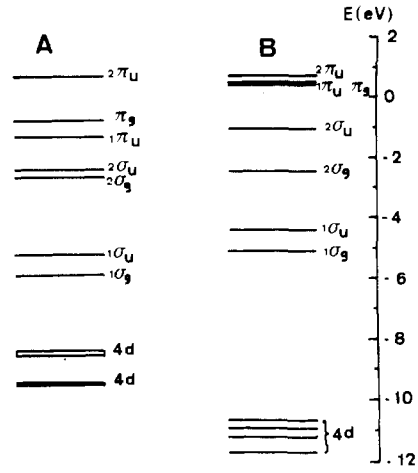

Figure 1. Calculated energy level diagrams of Ag_3: (A) Ag functions with 5s and 5p exponents respectively equal to 1.70 and 1.72; (B) Ag^+ functions.

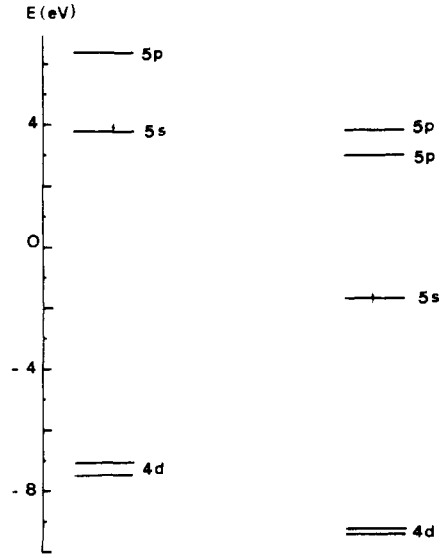

Figure 2. Calculated energy level diagrams of $[Ag(OH_2)_6]^0$ (left) and $[Ag(OH_2)_3]^0$ (right).

5p Slater-type functions equal to respectively 1.70 and 1.72. In Figure 1B the Ag^+ functions were used. The calculated transition energies are shown in Table II. These data confirm the assignment of the 2.59-eV band as the $^2\Sigma_u^+ \rightarrow {}^2\Sigma_g^+$ transition. We could not calculate a triplet in the 4.67–4.98-eV region. But from the data of Table II likely candidates are the transitions $1\sigma_g \rightarrow 2\sigma_u$, $1\sigma_u \rightarrow \pi_g$, and $1\sigma_g \rightarrow 1\pi_u$. The calculated charges on the atoms are given in Table III. It is important to note—for comparison with calculations on zeolitic clusters—the small negative charge on the central Ag, compensated by the positive charge on the external Ag atoms. The same charge distribution was obtained by Gellens et al. with an extended Hückel calculation.[10]

2. Zeolitic Clusters. When Ag, Ag_2, or Ag_3 is placed in an environment of H_2O molecules (to simulate the zeolitic environment), calculations with Ag functions fail to reproduce the observed visible absorption bands. This is expected: the outer orbitals, 5s and 5p, are interacting with the surrounding oxygens. They are contracted, resembling more Ag^+ orbitals than Ag orbitals. Therefore, in the following paragraphs only the results of the calculations with Ag^+ functions will be presented.

(a) $[Ag(OH_2)_6]^0$: Model 1. The energy levels of Ag in the hexagonal prism are shown in Figure 2. The calculated 5s–5p energy separation is 3.59 eV. A band at 3.73 eV has been assigned to Ag^0 in site I. Our calculation shows that this is a resonable assignment. The charge on Ag is 0.097–. The orbitals, designated 5s and 5p in Figure 2, have respectively 96% 5s character and 99% 5p character. The interaction with water molecules is therefore very small.

The calculation on Ag in site I′, $[Ag(OH_2)_3]^0$, splits the three p levels because of the decrease in symmetry and puts the 5s–5p energy separations at 4.69 and at 5.55 eV (Figure 2). We conclude that this model is less adequate to explain the 3.73-eV band.

(b) $[Ag_2(OH_2)_6]^{0,+}$: Model 2. This model applies only for zeolites X and Y. We are therefore looking for an absorption band at 3.10 eV. The interesting parts of the energy level diagrams are shown in Figure 3. As for model 1 and in agreement with the extended Hückel calculations[10] the interaction of the 5s and 5p orbitals of Ag with the H_2O molecules is very small. We have therefore designated the orbitals in Figure 3 by the Ag orbital symbols. Figure 3 shows that the MO's of Ag on site I, coordinated to six OH_2 groups, are significantly destabilized with respect to the MO's of Ag on site I′, coordinated to three OH_2 groups. This is especially the case for the charged cluster. There are two consequences: (i) A low-energy transition is produced at 2.23 eV as a charge transfer of an electron from a MO with primarily 5s character of Ag(I′) to a MO with primarily 5s character of Ag(I). (ii) The unpaired electron is mainly localized on Ag(I′). Thus Ag(I) formally behaves as Ag^+ and Ag(I′) as Ag^0 in the cluster $[Ag_2(OH_2)_6]^+$. The calculated atomic charges are given in Table IV.

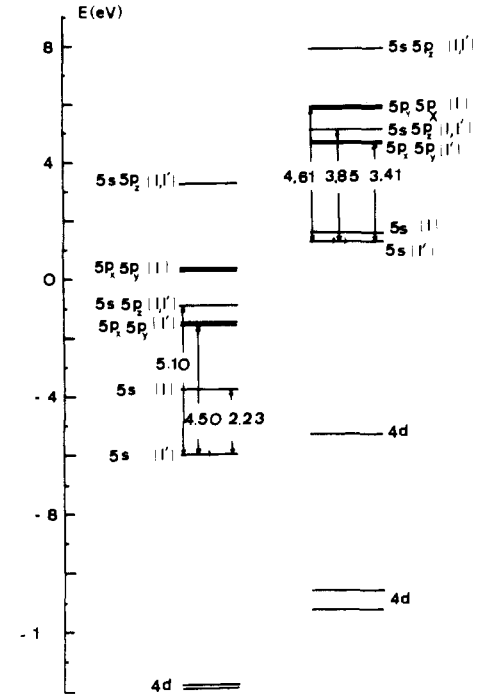

Figure 3. Calculated energy level diagrams of $[Ag_2(OH_2)_6]^0$ (right) and $[Ag_2(OH_2)_6]^+$ (left). Energy differences are indicated in eV.

Table IV. Atomic Charges of $[Ag_2(OH_2)_6]^{0,+}$ Cluster

atom	charge $[Ag_2(OH_2)_6]^0$	charge $[Ag_2(OH_2)_6]^+$
Ag(I′)	0.75–	0.01–
Ag(I)	0.50+	0.67+
O(I′,I)[a]	0.36–	0.39–
O(I)[b]	0.41–	0.40–
H	0.21+	0.23+

[a] Oxygen coordinated to Ag(I) and Ag(I′). [b] Oxygen coordinated to Ag(I) only.

Table V. Atomic Charges in $[Ag_3(OH_2)_6]$

cluster	overall charge	atomic charges Ag(I') (external Ag)	Ag(I) (central Ag)	O	H
$[Ag_3(OH_2)_6]$ (model 3)	0	0.49−	0.67+	0.38−	0.21+
	1+	0.01−	0.66+	0.39−	0.23+
	2+	0.45+	0.65+	0.40−	0.24+
$[(H_2O)_3Ag_3(OH_2)_3]$ (model 4)	0	0.10−	0.52−	0.30−	0.21+
	1+	0.23+	0.30−	0.30−	0.22+
	2+	0.38+	0.24+	0.29−	0.23+

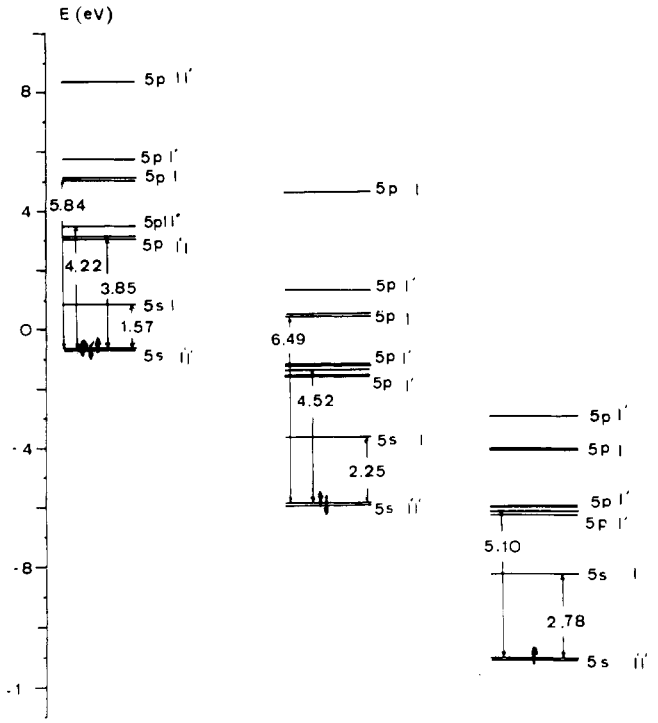

Figure 4. Calculated energy level diagrams of $[Ag_3(OH_2)_6]$ (model 3) with charge 0 (left), 1+ (middle), and 2+ (right). Energy differences are indicated in eV. I denotes central Ag or Ag on site I; I' denotes external Ag or Ag on sites I'.

(c) $[Ag_3(OH_2)_6]^{0,+,2+}$: Model 3. This model also applies to faujasite-type zeolites only. If differs from model 2 in that an additional Ag is positioned in site I'. Again we are interested in the low-energy transition at 3.10 eV. The calculated energy level diagrams are shown in Figure 4. The main atomic character of the levels is indicated. As for $[Ag_2(OH_2)_6]$, the energy level diagrams of Figure 4 indicate that a low-energy Ag(I') → Ag(I) charge transfer is generated, which is a likely candidate for the 3.10-eV band. The energy of this transition increases from 1.57 to 2.78 eV when the charge of the cluster increases from 0 to 2+. The calculations predict three to four transitions in the UV region. We do not discuss them in detail because of the lack of experimental data to compare them. Again, the Ag with the highest coordination number is electron deficient and carries a positive charge of (0.66 ± 0.01)+, whatever the overall charge of the cluster (Table V). The important difference with model 2 is that the HOMO is degenerate. The two levels 5s(I') + 5s(I') and 5s(I') − 5s(I') have the same energy. For $[Ag_3(OH_2)_6]^+$ this energy is exactly that of the 5s(I') level in $[Ag_2(OH_2)_3]^+$ (Figure 3). Also, the 5s(I) levels of both clusters have the same energy. This shows that the two external Ag's of $[Ag_3(OH_2)_6]$ are too far apart (~0.620 nm) to interact with each other. All the MO's involving the 5s and 5p orbitals of Ag have at least 93% Ag character. Table VI–VIII contain the exact numbers.

Table VI. Character of MO's of $[Ag_3(OH_2)_6]^0$ (Model 3)

MO	energy/eV	percent character Ag (I') 5s	Ag (I') 5p	Ag(I) 5s	Ag(I) 5p	Ag(I') 5s	Ag(I') 5p	O
40	−0.72	45.2	4.8	0.0	0.0	45.1	4.8	0.0
41	−0.70	44.1	4.9	1.3	0.0	44.1	4.9	0.0
42	0.87	0.0	3.8	85.8	0.0	0.0	3.8	6.1
43, 44	3.15	0.0	40.8	0.0	17.8	0.0	40.8	0.6
45	3.52	2.5	28.4	0.0	37.7	2.5	28.4	0.4
46, 47	3.58	0.0	50.0	0.0	0.0	0.0	50.0	0.0
48, 49	5.14	0.0	9.2	0.0	80.3	0.0	9.2	2.1
50	5.77	5.9	41.5	3.6	0.0	5.9	41.5	1.2
51	8.38	1.9	16.9	0.0	59.9	1.9	16.9	2.0

Table VII. Character of MO's of $[Ag_3(OH_2)_6]^+$ (Model 3)

MO	energy/eV	percent character Ag(I') 5s	Ag(I') 5p	Ag(I) 5s	Ag(I) 5p	Ag(I') 5s	Ag(I') 5p	O	H
40	−5.97	51.1	5.2	0.0	0.0	38.8	4.0	1.0	0.0
41	−5.96	37.7	4.0	1.8	0.0	50.1	5.2	1.2	0.0
42	−3.71	0.0	6.5	80.6	0.0	0.0	6.5	6.3	0.2
43, 44	−1.58	0.0	43.8	0.0	12.1	0.0	43.6	0.5	0.0
45	−1.44	2.0	29.6	0.0	35.9	2.0	29.6	0.8	0.0
46, 47	−1.26	0.0	49.9	0.0	0.0	0.0	50.2	0.3	−0.1
48, 49	0.53	0.0	6.3	0.0	85.9	0.0	6.3	2.0	−0.4
50	1.34	5.6	39.0	8.3	0.0	5.6	39.0	1.9	0.0
51	4.66	2.2	15.8	0.0	61.6	2.2	15.8	1.9	0.0

Table VIII. Character of MO's of $[Ag_3(OH_2)_6]^{2+}$ (Model 3)

MO	energy/eV	percent character Ag(I') 5s	Ag(I') 5p	Ag(I) 5s	Ag(I) 5p	Ag(I') 5s	Ag(I') 5p	O
40	−11.17	72.6	7.3	2.0	0.0	14.6	1.5	1.8
41	−11.16	15.5	1.5	0.0	0.0	73.4	7.4	1.7
42	−8.38	0.0	9.1	75.4	0.0	0.0	9.1	6.4
43	−6.39	1.6	30.2	0.0	35.1	1.6	30.1	1.2
44, 45	−6.32	0.0	46.3	0.0	8.4	0.0	44.6	0.7
46, 47	−6.07	0.0	48.9	0.0	0.0	0.0	50.7	0.5
48, 49	−4.11	0.0	4.3	0.0	83.3	0.0	4.3	2.3
50	−3.00	5.5	36.4	12.9	0.0	5.5	36.4	2.5
51	0.93	2.5	15.2	0.0	62.1	2.5	15.3	2.0

(d) $[(H_2O)_3Ag_3(OH_2)_3]^{0,+,2+}$: Model 4. This model refers to the Ag_3 cluster in yellow zeolite A with a low-energy absorption band at 2.85 eV. We did not calculate the Ag_6 cluster in this system with an observed absorption band at 2.48 eV, because the energy difference with the Ag_3 cluster is too small to be significantly calculated with our method. The energy level diagrams are shown in Figure 5. The main character of the MO's is indicated in the figure, but exact numbers can be found in Table IX–XI. All the MO's containing 5s and 5p atomic orbitals have at least 90% Ag character. The atomic charges are given in Table V. The most important feature of Figure 5 is a low-energy transition from a MO essentially localized on the central Ag to a MO mainly localized on the external Ag atoms. This energy separation increases with

Table IX. Character of MO's of $[(H_2O)_3Ag_3(OH_2)_3]^0$ (Model 4)

		percent character							
		Ag external		Ag central		Ag external			
MO	energy/eV	5s	5p	5s	5p	5s	5p	O	H
40	−1.40	9.6	6.4	65.4	0.0	9.7	6.5	0.3	0.0
41	−0.38	22.2	15.8	0.0	23.0	22.2	15.8	0.8	0.0
42, 43	3.69	0.0	0.0	0.0	100.2	0.0	0.0	0.0	0.0
44	5.06	22.9	7.7	33.3	0.0	22.9	7.7	1.6	0.0
45, 46	9.33	0.0	45.3	0.0	0.0	0.0	48.7	5.2	−0.7
47, 48	9.41	0.0	48.7	0.0	0.0	0.0	45.3	4.2	−0.8
49	11.12	19.1	−2.2	0.0	61.7	19.1	−2.2	3.6	0.0
50	16.84	12.8	33.7	0.0	0.0	12.8	33.7	6.9	−0.2
51	18.28	5.1	35.8	0.0	13.9	5.1	35.7	4.5	0.0

Table X. Character of MO's of $[(H_2O)_3Ag_3(OH_2)_3]^+$ (Model 4)

		percent character						
		Ag external		Ag central		Ag external		
MO	energy/eV	5s	5p	5s	5p	5s	5p	O
40	−6.80	9.4	6.5	65.6	0.0	9.4	6.5	0.5
41	−5.74	20.2	14.9	0.0	28.3	20.2	14.9	1.0
42, 43	−1.73	0.0	0.0	0.0	100.0	0.0	0.0	0.0
44	0.78	23.3	7.4	32.8	0.0	23.4	7.4	2.0
45, 46	4.56	0.0	47.5	0.0	0.0	0.0	47.5	5.8
47, 48	4.67	0.0	45.7	0.0	0.0	0.0	47.4	5.9
49	7.00	22.5	−1.6	0.0	52.4	22.5	−1.6	5.0
50	12.27	12.1	33.8	0.0	0.0	12.1	33.8	8.0
51	14.15	3.1	35.8	0.0	17.5	3.1	35.8	4.6

Table XI. Character of MO's of $[(H_2O)_3Ag_3(OH_2)_3]^{2+}$ (Model 4)

		percent character						
		external Ag		central Ag		external Ag		
MO	energy/eV	5s	5p	5s	5p	5s	5p	O
40	−13.31	7.0	5.3	72.5	0.0	7.0	5.2	0.5
41	−11.34	17.3	13.6	0.0	36.2	17.3	13.6	1.0
42, 43	−7.81	0.0	0.0	0.0	99.8	0.0	0.0	0.0
44	−3.41	26.6	8.2	24.5	0.0	26.6	8.2	2.7
45, 46	−0.15	0.0	46.4	0.0	0.0	0.0	45.9	6.8
47, 48	0.00	0.0	45.8	0.0	0.0	0.0	46.3	6.9
49	2.65	26.2	−1.1	0.0	42.3	26.2	−1.1	6.5
50	7.83	10.9	34.4	0.0	0.0	10.9	34.4	9.1
51	10.12	1.6	36.4	0.0	19.1	1.6	36.4	4.7

increasing overall positive charge on the cluster from 1.02 to 1.97 eV (see also model 3). The energy level diagram follows the general rule that the orbitals of the atom with the smallest coordination number are lowest in energy. In this case, it is the central Ag. The low-energy charge transfer is therefore in the reversed direction as compared to that of model 3. Thus the HOMO is nondegenerate and the central Ag carries excess negative charge (Table V). This charge distribution is also the reverse of that of model 3. The change is brought about by the difference in coordination of the Ag atoms in the two models. In any case, the calculated low-energy Ag–Ag charge-transfer transition is a likely candidate for the observed 2.85-eV band.

Discussion

The Fenske–Hall SCF molecular orbital calculations with Ag^+ functions on model Ag clusters allow a qualitative explanation of the characteristic, visible absorption bands of Ag–zeolites. These models are derived from experimental structural data. The link between the structural data and spectroscopic data has therefore been given by this work. The characteristic transitions are between MO's with more than 90% 5s and/or 5p character of Ag. The same result is obtained by Gellens et al.[10] with an extended Hückel calculation including SiO_4 and AlO_4 tetrahedra. Therefore, our approximation of the zeolitic lattice by H_2O molecules is justified.

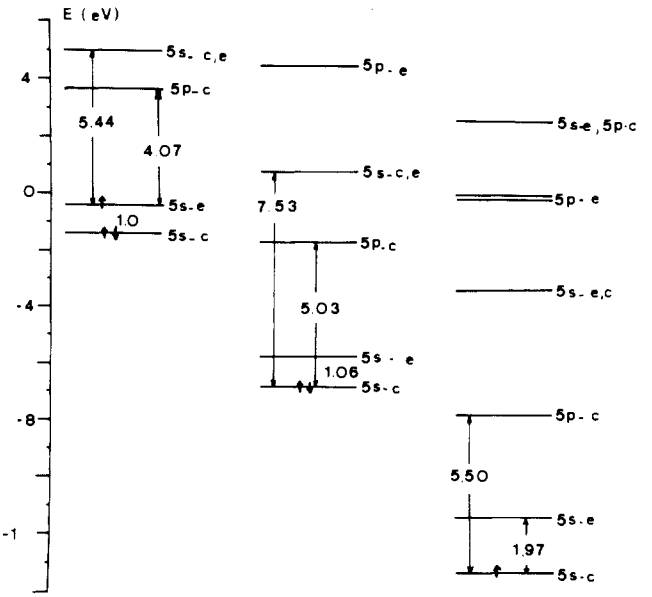

Figure 5. Calculated energy level diagrams of $[(H_2O)_3Ag_3(OH_2)_3]$ (model 4) with charge 0 (left), 1+ (middle), and 2+ (right). Energy differences are indicated in eV; c = central Ag, e = external Ag.

For faujasite-type zeolites the 3.73-eV band is adequately described as a 5s–5p transition of Ag^0 in site I, as proposed in the literature.[7-9,11] The difficulty with the $[Ag(OH_2)_6]^0$ model is that a certain amount of paramagnetism and a Ag^0 EPR signal are expected. The latter has not been observed until now.[20] It is therefore impossible to exclude entirely neutral, polynuclear clusters as being responsible for the 3.73-eV absorption. For electrostatic reasons they are expected to be less stable and less probable.

The 3.10-eV band of yellow faujasite-type zeolites is ascribed to transitions between MO's, primarily composed of 5s atomic orbitals of Ag. On the basis of the calculations no distinction can be made between $[Ag_2(OH_2)_6]^{x+}$ (model 2) and $[Ag_3(OH_2)_6]^{x+}$ (model 3) clusters. Also, the overall cluster charge is not unambiguously established. A neutral cluster is unlikely to be stable, because the zeolitic lattice is negatively charged. There remain then three possible clusters, $[Ag_2(OH_2)_6]^+$, $[Ag_3(OH_2)_6]^+$, and $[Ag_3(OH_2)_6]^{2+}$, as candidates for the 3.10-eV band.

However, Ozin and Huges[9,11] recently observed an absorption band at 3.65–3.45 eV for Ag–zeolites and ascribed it to Ag_2^+ clusters. The 3.10-eV band grows in the spectra at the expense of the 3.65–3.45-eV band and was therefore ascribed to Ag_3^{2+}. Our calculations are not accurate enough to distinguish between these two clusters. But, we favor the formulation of the trinuclear cluster as $[Ag_3(OH_2)_6]^+$. Indeed,

(20) Hermerschmidt, D.; Haul, R. *Ber. Bunsenges. Phys. Chem.* **1980**, *84*, 902.

Beyer and Jacobs[21] observed a three-step reduction of Ag^+ in chabazite corresponding to 50%, 66%, and 100% reduction. This corresponds to the formation of respectively Ag_2^+, Ag_3^+, and a completely reduced Ag–chabazite. For the charged clusters the Ag^+ ion was supposed to be located in the hexagonal prism of chabazite (analogous to site I in faujasite-type zeolites). This charge distribution follows the common coordination chemistry knowledge that the most highly charged cations tend to have the highest coordination number (in the present case 6 for Ag^+ and 3 for Ag^0). Thus both the dinuclear and trinuclear clusters can formally be represented Ag^0–Ag^+ and Ag^0–Ag^+–Ag^0 with Ag^+ on site I, coordinated to six oxygens, and Ag^0 and site I′, coordinated to three oxygens.

Ozin et al.[11] proposed an alternative interpretation of the 3.10-eV band of trinuclear clusters. They ascribed it to a transition from filled d-type valence levels to the half-filled s-type level of Ag_3^{2+}. This proposal was made on the bais of $X\alpha$ calculations on naked clusters. It seems that more extensive calculations with inclusion of the zeolitic environment are necessary to distinguish between our interpretation and Ozin's.

The description of the Ag_3 cluster in zeolite A (model 4) follows the same lines as exposed for the dinuclear and trinuclear clusters in zeolite X and Y. Thus, a neutral cluster is unlikely to occur because of the negatively charged framework of the zeolite. The two external Ag's are coordinated to lattice oxygens. They are expected to carry the positive charge, and a cluster, formally represented as Ag^+–Ag^0–Ag^+, seems to be the most reasonable formulation. This has been proposed already in the literature.[3] As for the yellow zeolites X and Y, the visibile absorption band of yellow zeolite A is due to a charge transfer, but now from a MO mainly localized on the central Ag to a MO localized on the external Ag atoms. This cluster carries an unpaired electron. We have been able to measure a small amount of paramagnetism on the yellow and brick red AgA zeolites, which have the characteristic absorptions at 2.85 and 2.48 eV, respectively.[3] If the magnetic moment of Ag^0 is taken as the spin-only value of 1.75 μ_B, the experimental magnetic moment corresponds to 0.7 Ag^0 and 1.2 Ag^0 per unit cell for yellow and brick red AgA, respectively. These numbers are two times smaller than these obtained from X-ray diffraction studies.[3] In any case these experiments show that a small amount of paramagnetic Ag species are likely to be present in yellow and brick red AgA.

An interesting problem arises about the geometry of these positively charged, trinuclear clusters. For the free clusters, Ag_3^+ or Ag_3^{2+}, the most stable configuration is the equilateral triangle.[13] In zeolites, the clusters are linear or nearly so. It must be that the zeolite lattice imposes strong constraints on the construction of metallic clusters. It is worth mentioning that they are destroyed by treatment with H_2 and H_2O but not by an O_2 treatment.[4,7] This may be a consequence of the fact that H_2 and H_2O can penetrate the cubooctahedra but O_2 cannot or at least can only with great difficulty.

Conclusions

The spectroscopic properties of Ag clusters in zeolites are explained with the cluster models proposed in the literature on the basis of X-ray diffraction data. The absorption band of Ag^0 in site I is a 5s–5p transition. The yellow color of zeolites X and Y is due to a charge transfer from a MO on Ag in I′ to a MO on Ag in I. The cluster can be Ag_2 or Ag_3, and the most likely charge is 1+. The positive charge is carried by Ag in I. The yellow color of zeolite A is due to a charge transfer from the central Ag to the external Ag atoms of the Ag_3 clusters. The most likely formulation of this cluster is Ag^+–Ag^0–Ag^+. The linear geometry of all these clusters is imposed by the zeolitic framework.

Acknowledgment. R.A.S. acknowledges the National Fund of Sciencific Research (Brussels, Belgium) for a position as Senior Research Associate and a short-stay grant to perform this research. This work was partially supported by the National Science Foundation under Grant no. CHE-8112893.

Registry No. Ag, 7440-22-4; Ag_2, 12187-06-3; Ag_3, 12595-26-5.

(21) Beyer, H. K.; Jacobs, P. A. In "Metal Microstructures in Zeolites"; Jacobs, P. A., Jaeger, N. I., Jiru, P., Schulz-Ekloff, G.; Eds.; Elsevier: Amsterdam, 1982; p 95.

Contribution from the Department of Chemistry, Calvin College, Grand Rapids, Michigan 49506

MNDO Studies of Proton Affinity as a Probe of Electronic Structure. 1. General Overview

ROGER L. DeKOCK* and CRAIG P. JASPERSE

Received August 16, 1982

MNDO calculations have been performed on 43 molecules and ions and their protonated counterparts. The calculated proton affinities give a mean error of 8%, in comparison to available experimental results. The calculated structures of the protonated molecules agree well with experiment and/or ab initio LCAO–SCF–MO theory. Extensive charge redistribution is brought about by protonation of a substrate molecule. Generally the proton receives electron density from regions of the molecule far removed from the site of attack. Both the frontier orbital theory and calculated atomic charges serve as useful guidelines to predict the site of proton attack in molecules such as CO, NH_3, HNCO, N_2O, ketene, and furan. The most stable site of attack also gives the proton the most electron density in these protonated molecules. A crude correlation exists between calculated ionization energy and proton affinity. A correlation also is found between the final atomic charge on the attacking proton and the proton affinity. The MNDO method underestimates the alkyl substituent effect but overestimates the fluoro substituent effect on proton affinity. This has adverse effects in the use of MNDO to calculate the site of proton attack in perfluoro compounds such as NF_3.

Introduction

Experimental studies of proton affinity have advanced rapidly over the last 15 years, particularly with the advent of ion cyclotron resonance spectroscopy.[1,2] At the same time theoretical studies[3] have provided insight into the energetics of protonation and into the geometrical changes and charge

(1) Beauchamp, J. L. *Annu. Rev. Phys. Chem.* **1971**, *22*, 527. Kebarle, P. *Ibid.* **1977**, *28*, 445.

0020-1669/83/1322-3839$01.50/0